Binding Thermodynamics and Kinetics Calculations Using Chemical Host and Guest: A Comprehensive Picture of Molecular Recognition

Zhiye Tang and Chia-en A. Chang*

Department of Chemistry, University of California, Riverside, CA92521

Telephone: (951) 827-7263

Email: chiaenc@ucr.edu

Understanding the fine balance between changes of entropy and enthalpy and the competition between a guest and water molecules in molecular binding is crucial in fundamental studies and practical applications. Experiments provide measurements. However, illustrating the binding/unbinding processes gives a complete picture of molecular recognition not directly available from experiments, and computational methods bridge the gaps. Here, we investigated guest association/dissociation with β-cyclodextrin (β-CD) by using microsecond-timescale molecular dynamics (MD) simulations, post-analysis and numerical calculations. We computed association and dissociation rate constants, enthalpy, and solvent and solute entropy of binding. All the computed values of k_{on}, k_{off}, ΔH, ΔS, and ΔG could be compared with experimental data directly and agreed well with experiment findings. Water molecules play a crucial role in guest binding to β-CD. Collective water/β-CD motions could contribute to different computed k_{on} and ΔH values by using GAFF-CD and q4MD-CD force fields for β-CD, mainly because of the motion of β-CD that provides different hydrogen-bond networks of water molecules in the cavity of free β-CD and the strength of desolvation penalty. Both force fields resulted in similar computed ΔG from independently computed kinetics rates and thermodynamics properties (ΔH, ΔS), enthalpy-entropy compensation and the same driving forces of binding, non-polar attractions between solutes and entropy gain of desolvating water molecules. However, the balances of ΔH and -TΔS are not identical. The study further interprets experiments, deepens our understanding of ligand binding, and suggests strategies for force field parameterization.

Keywords: protein-ligand binding affinity; cell method; drug design; H-bond, hydration shell dynamics

Significance Statement

Building a more complete picture of molecular recognition requires an examination of the entire binding/unbinding processes and driving forces in atomistic details. Therefore, we used unbiased microsecond molecular dynamics (MD) simulations to study β-cyclodextrin (β-CD) and guests binding/unbinding, a host-guest system of great theoretical interest and practical applications. We modeled the association/dissociation pathways and their rates k_{on} and k_{off}, and showed that the competition between a guest and waters during the binding process slows down k_{on}. We revealed that waters induce β-CD motions and contribute to the balance of entropy and enthalpy changes upon guest binding. The new findings about hydrophobicity and entropy for the solvent, guests and β-CD during recognition may also be general in weak binding ligand-protein systems.

Molecular recognition determines binding of molecules — a common phenomenon in chemical and biological processes. Thus, understanding molecular recognition is of interest in fundamental studies and also has practical applications in chemical industries and drug discovery. Binding affinity is a straightforward characterizer of recognition and can be obtained experimentally by measuring enthalpy-temperature series with methods such as calorimetry (1, 2). However, it is difficult to measure the binding entropy directly from experiments, and it is impossible to differentiate solute and solvent entropies. Recent studies have revealed the importance of kinetic properties (3-5) such as residence time and showed that drug efficacy is sometimes correlated with the kinetic properties better than binding affinity (6, 7). With recent technical breakthroughs, molecular dynamics (MD) is able to simulate up to millisecond timescale molecular motions with the advantage of atomistic resolution (8). Therefore, computational methods can be used to sample a larger time scale of unbiased dynamics and extract the enthalpic and entropic profiles of both the solvent and solute, as well as the kinetics. New findings observed from chemical host–guest systems have advanced our knowledge of molecular recognition and brought new insights into ligand–protein systems.

β-Cyclodextrin (β-CD) is a cyclic oligosaccharide compound that can be obtained by degradation of starch by α-1,4-glucan-glycosyltransferases. β-CD (Fig. 1) encloses a hydrophobic cavity with a diameter of about 6.5 Å while its rim consists of hydrophilic hydroxyl groups. Notably, the wide and narrow rims of β-CD are asymmetrical. Because of its structure and size, β-CD can host a wide variety of guest molecules. With these properties, β-CD and its derivatives have many applications in many fields, such as the cosmetic industry, pharmaceuticals, catalysis, and the food and agricultural industries (9), and experimental measurements are available for a variety of β-CD complexes (10-13). Accurate binding affinity calculations have been performed with implicit solvent using the M2 and BEDAM methods (14, 15). MD simulations and QM/MM methods have been used to study H-bonds, binding enthalpy and properties of β-CD complexes (16-20). With implicit solvent model, binding affinity can be decomposed into configuration entropy; however, lacking the solvent entropy component made it impossible to direct compare computation results with experimental measured ΔH and ΔS. Yet no modeling work on binding kinetics has successfully sampled multiple association/dissociation events for kinetic rate calculations.

The present study applied microsecond-timescale MD simulations to compute binding kinetics and thermodynamics of 7 guests with β-CD using GAFF-CD and q4MD-CD force fields. We computed k_{on} and k_{off} from the multiple binding/unbinding events in the MD of the complex. We also computed enthalpy and entropy of solute and solvents using simulations of free host and guest, the complex, and empty water

box. Surprisingly, the more complicated H-bond networks in the first hydration shell of free β-CD provided by GAFF-CD resulted in the differences of slower k_{on} and larger desolvation penalty, instead of different host-guest non-polar interactions. We also gave details about how enthalpy/entropy and van der Waals/Coulombic energies contribute to binding kinetics/thermodynamics and association/dissociation pathways.

Results

We used microsecond-timescale MD simulations with an explicit solvent model to compute the binding enthalpies, entropies, and association/dissociation rate constants for β-CD complexes. Although the 7 guest molecules all have weak binding affinities, we termed 1-butanol, t-butanol, 1-propanol, methyl butyrate as weak binders, and termed aspirin, 1-naphthyl ethanol, 2-naphthyl ethanol as strong binders (Fig. 1). All computed results yielded good agreement with experimental data (Tables 1 and 2, and Fig. S6). Two force fields, GAFF-CD and q4MD-CD, were used to assign parameters for β-CD, and all ligands used the GAFF force field. In general, GAFF-CD yield results agreed better with experimental measured kinetics and thermodynamics values.

Binding Enthalpy and Entropy Calculations

The calculated ΔH, -TΔS and ΔG_{Comp1} with the GAFF-CD and q4MD-CD force fields are compared with the experimental data in Table 1. The computed ΔG is mostly within 1.5 kcal/mol of experiments, and they provide a correct trend, although GAFF-CD generally underestimated and q4MD-CD overestimated the binding free energy. Two major driving forces of the complex formation are the intermolecular van der Waals (vdW) attraction between the β-CD and guest (Table S3 and S4) and water entropy gain on binding (Table 3). Interestingly, with GAFF-CD, the underestimated binding affinities are primarily from larger desolvation penalty, resulting in the less negative binding enthalpy. The host became more flexible and gained configuration entropy on binding, which is another favorable factor in guest binding (Table 3). In contrast, q4MD-CD modeled a significantly smaller desolvation penalty and more negative ΔH, which become the main driving force for binding. However, the systems need to pay a higher cost in entropy (–TΔS) because the host became more rigid in the bound state.

These results suggest entropy-enthalpy compensation in our systems with different force fields, so the compensation in these systems indeed has a physical implication and is not the artifact from mathematics of ΔG_{Comp1}= ΔH - TΔS. We compared the calculated ΔH and -TΔS for 1-propanol and 1-

butanol for which experimental data are available. Both experiments and calculations with GAFF-CD showed a small positive ΔH, which slightly opposed binding, but the systems gained more entropy to compensate losing enthalpy on binding. Although only 2 guests studied here have experimental ΔH and -TΔS, the binding data for other alcohols with β-CD using calorimetry (ITC) and UV experiments commonly show gaining entropy, and enthalpy was not the predominant determinant for binding in all cases (Fig. S7). As a result, computed binding enthalpy and entropy with GAFF-CD agreed better than with q4MD-CD, and details will be presented in the following subsections.

Changes of Enthalpy from Different Components. We evaluated the absolute values of binding enthalpy by using potential energies <E> from MD trajectories of the four species, and the convergences of the enthalpy calculations were first examined (Figs. S8 to S10). For all simulations, <E> reaches a stable value within a fluctuation of 0.4 kcal/mol, which is also within reported experimental uncertainty (10-12, 21, 22). The fluctuations of potential energies of β-CD complexes with 1–propanol, 1–butanol and t–butanol are larger with GAFF-CD than the other systems because the bound state fractions of these systems are lower than those with the other systems.

To understand binding enthalpies, we decomposed the calculated values into various contributions (Table S3). We also provide the decompositions into vdW and Coulombic interactions for $\Delta H_{\text{Solute Inter}}$, $\Delta H_{\text{Host Conf}}$, $\Delta H_{\text{Host-Water}}$ and $\Delta H_{\text{Guest-Water}}$ (Table 4 and Tables S4 and S5). Regardless of force field, we immediately noticed that $\Delta H_{\text{Host-Guest}}$ data are all favorable (negative), and strong binders have large negative $\Delta H_{\text{Host-Guest}}$ value, ~ -30 kcal/mol (Table S3). However, $\Delta H_{\text{Desolvation}}$ largely compensates $\Delta H_{\text{Host-Guest}}$, for significantly smaller ΔH, ranging from 3.0 to -1.4 kcal/mol with GAFF-CD and -0.9 to -5.7 kcal/mol with q4MD-CD. The computed ΔH with GAFF-CD yielded positive values for weak binders, which has been seen in experiments. In contrast, ΔH values are all negative with q4MD-CD. On binding, both β-CD and the guest desolvate water molecules; thus, $\Delta H_{\text{Host-Water}}$ and $\Delta H_{\text{Guest-Water}}$ values are all positive. The values are larger for strong binders presumably because of larger sizes. The water molecules released after binding regain interactions with other water molecules, thereby resulting in all negative $\Delta H_{\text{Water-Water}}$ values. However, this term is not negative enough to counterbalance $\Delta H_{\text{Host-Water}}$ and $\Delta H_{\text{Guest-Water}}$. As a result, desolvation enthalpy is inevitably all positive and becomes the major force that opposes binding. Surprisingly, $\Delta H_{\text{Solute Inter}}$ and its vdW and Coulombic decompositions (Table S4) are similar in both force fields, and it is the Coulombic term of $\Delta H_{\text{Host-Water}}$ that contributes to the stronger desolvation penalty modeled with GAFF-CD (Table 4). As illustrated in Fig. 2 and Table S8, the two force fields

modeled different β-CD conformations, and β-CD needs to break more intermolecular H-bonding to pay larger desolvation penalty in GAFF-CD on guest binding.

After losing intermolecular H-bonds on guest binding, β-CD regained the intramolecular Columbic attraction in the bound state ($\Delta H_{\text{Host Conf (Coul)}}$ in Table S5). Although the values of $\Delta H_{\text{Host-Guest}}$ with both force fields are similar, the decomposition shows significantly larger numbers of $\Delta H_{\text{Host Conf (vdW)}}$ and $\Delta H_{\text{Host Conf (Coul)}}$ with GAFF-CD (Table S5) because of larger conformational changes after ligand binding. With GAFF-CD, the free β-CD prefers flipping 2 glucopyranose units instead of holding an open cavity as in the crystal structure (Fig. 3). The glucose rings flipped outward during ligand binding, which lost more water molecules to allow the guest access to the β-CD binding site. In contrast, q4MD-CD appeared to have crystal-like host structures in both the free and bound states. Note that in vacuum, both GAFF-CD and q4MD-CD sampled predominantly crystal-like host structures (Fig. S12), which indicates that the glucose ring flipping is largely induced by the hydration shell. GAFF-CD not only changed host conformations upon ligand binding, but also makes the host more flexible.

Changes of Solute Entropy on Ligand Binding. Solute entropy, also termed configuration entropy, reflects the flexibility of a molecular system. Here we used numerical integration to compute solute entropy terms, using equations shown in SI for internal (conformational/vibrational) and for external (translational/rotational). Well-defined dihedral distribution analyzed from our MD trajectories is used to compute internal solute entropy, as detailed in SI Section 1. The entropy terms were computed separately because external and internal degrees of freedom do not correlate with each other. The calculated entropy values are shown in Table 3. A system is well known to lose configuration entropy because the intermolecular attractions inevitably rigidify the 2 molecules on binding (14, 15, 23). For example, a tight binder may lose ~ 7 kcal/mol external entropy by confining itself in a snug binding site as compared with freely translating and rotating itself in a space equivalent to 1 M standard concentration (24). Post-analyzing our MD trajectories showed that all guests and β-CD were not markedly rigidified in the bound state. The guests lost ~ 1.5–2 kcal/mol external entropy, and β-CD was slightly more flexible, gaining 0.5–1.8 kcal/mol internal entropy with GAFF-CD or being unchanged with q4MD-CD on guest binding (Table 3). The variation in internal entropy of guests ($-T\Delta S_{\text{Guest Int}}$) is negligible because the guests are small and rigid molecules. Intuitively, a stiffer host in the bound complex is likely to rigidify the guest as well because the 2 molecules are moving in concert. However, for the small and weak binding guests studied here, the interactions between β-CD and guests are not large enough to strongly confine a guest to

a handful of well-defined bound guest conformations. Thereby, the guest can freely tumble and diffuse in the cavity of β-CD, resulting in a small reduction of $-T\Delta S_{Guest\ Ext}$ (Fig. S13 and SI Movie).

Changes of Water Entropy on Ligand Binding. Water entropy is one major driving force in ligand binding in these systems, contributing to -2 to -4 kcal/mol to the free energy of binding (Tables 1 and 3). Gaining water entropy dominates in the binding of all guests to β-CD with GAFF-CD and the first 3 weak binders to β-CD with q4MD-CD. The change in water entropy ($-T\Delta S_{water}$) is a combined effect from rearranging water molecules, which affects their vibrational and conformational entropy, and from releasing the water molecules residing in the cavity of β-CD or interacting with the guest after the complex is formed (Tables S6 and S9 to S11). We first validated use of a grid cell theory and TIP3P model by comparing our computed molar entropy of bulk water, 73.80 J/mol/K (Tables S9 to S11), with standard molar entropy of water, 69.95 kcal/mol. In general, our computed solvent entropy showed that the translational entropy decreases at the surface of the solute because the existence of the solute hinders free diffusion of water molecules, and the rotational entropy increases on the hydrophobic surface and decreases near hydrophilic regions. The water entropy fluctuation around solutes is visualized in Fig. S14. Aspirin and methyl butyrate have more water entropy gains on binding because they have more polar functional groups to capture nearby water molecules in their free state, and after forming the complex with β-CD, these water molecules are released. Notably, using different force fields for β-CD did not change the computed $-T\Delta S_{Water}$, so solute flexibility does not play an important role in water entropy calculations.

Binding Kinetics: Calculations of Association and Dissociation Rate Constants

The fast kinetics of guest binding to β-CD allowed for directly assessing the association (k_{on}) and dissociation (k_{off}) rate constants from the bound and unbound lengths during microsecond-long unguided MD simulations (Table 2). The estimated diffusion-controlled association rate constants ($k_{on\_diffuse}$) for all systems are ~ 3–4×10^{10} $M^{-1}s^{-1}$ approximated by $k_{on\_diffuse} = 4\pi DR$ (SI Section 12). The modeled k_{on} by using GAFF-CD agrees very well with experimental data, and all guests showed 2 orders of magnitude slower k_{on} than $k_{on\_diffuse}$. Using q4MD-CD slightly overestimated k_{on} for all guest binding, and the value is one order of magnitude slower than $k_{on\_diffuse}$ because of the spatial factor. Because β-CD does not require considerably conformational changes or slow transition to acquire all the guests, experiments revealed no differences in k_{on} for different guests. However, k_{on} modeled with GAFF-CD shows that strong binders associate marginally faster to β-CD, with k_{on} values close to 10^9 $M^{-1}s^{-1}$, as compared with

weak binders, with k_{on} ~ 2–3×10^8 $M^{-1}s^{-1}$. In contrast, because k_{on} modeled with q4MD-CD is already fast and close to $k_{on\_diffuse}$, a small difference is observed, with k_{on} ~ 1–4×10^9 $M^{-1}s^{-1}$.

The difference in computed k_{on} with the two force fields and from experimental k_{on} result from the intermolecular attractions and the desolvation process. β-CD features a restricted target area which is window areas of the cavity, ~ 2.5% of the entire surface. When no guests diffusing on the β-CD surface, successful binding occurs only with the first collision occurring in the target area. With q4MD-CD, modeled k_{on} is 20 times slower than $k_{on\_diffuse}$, and ~ 5% of molecular encounters result in successful binding. Therefore, the restricted target area is the main contribution to a slower k_{on}. Using the same concept, less than 1% of the initial association results in a stable complex modeled with GAFF-CD, except for aspirin and 2-naphthyl ethanol. We found that the desolvation process further slowed down k_{on}. Although the tilt glucose rings in the free β-CD may partly occlude the cavity, rotating the 2 dihedrals in C-O-C for different glucose ring tilting is nearly barrier-less. Replacing water molecules that formed the H-bond network with the free β-CD creates an energy barrier and results in unsuccessful binding, even for a guest already diffused to the target area. Note, successful binding was considered only when a complex formed > 1 ns during MD simulations.

In contrast to k_{on}, k_{off} modeled by q4MD-CD agrees very well with experiments; however, with GAFF-CD, almost all guests left β-CD approximately one order faster than the measured k_{off} values. Because of the faster k_{off}, the equilibrium constants (K_{eq}) are systematically smaller than the experimental values. The dissociation rate constants are directly proportional to how long a guest can stay in the pocket of β-CD, also termed residence time in the drug discovery community. Different force field parameters can largely affect k_{off}. The longer average bound time corresponds to more negative ΔH (Table S3) with q4MD-CD than that with GAFF-CD. However, longer bound time does not always require stronger intermolecular attractions, and Table 3 shows that the water effects can be the major differentiating factors. Of note, although we sampled several bound/free states during long simulations (Tables S13 and S14), real experiments averaged hundreds of such events. As a result, reaching a full convergence calculations may be challenging for tight binders, and significantly longer simulation is necessary.

For the weak binders, we observed one direct association/dissociation pathway in which a guest diffused into the window of the cavity and then stayed with β-CD. The association perturbed the conformations of β-CD to get rid of hydrated waters and flip glucopyranose. We term this pathway the direct binding pathway (SI Movies 1,2,7,8). For the strong binders such as aspirin, for which k_{on} is 3- to 10-fold faster than weak binders modeled by both force fields, we observed one more

association/dissociation pathway, termed the sticky binding pathway (SI Movies 3-6, 9-12). The stronger intermolecular attractions allow the guest to stay on the surface of β-CD for surface diffusion to reach the cavity. This situation largely increases the possibility of binding events because the guests can overcome the limitation of a restricted target area of the surface. Note that unlike some ligand–protein binding in which the large biomolecular system needs longer than a microsecond timescale for both molecules to arrange to form a complex, binding processes of guest–β-CD are very fast, in the sub-nanosecond range, without large energy barriers. Nevertheless, the intermolecular attractions, possible surface diffusion and desolvation process still play a key role in controlling binding kinetics.

Discussion

This study demonstrates that unbiased MD simulations can be used to compute CD–guest binding kinetics and thermodynamics with various numerical post-analysis. Computed values with GAFF-CD and q4MD-CD both agree well with experimental measures; however, values strikingly differ depending on whether the binding is driving by ΔH or ΔS. Intuitively, a more negative ΔH modeled by q4MD-CD is likely a result of the Lennard-Jones parameters, which could result in more optimized $\Delta H_{\text{Host-Guest}}$ (25). Nevertheless, in the decomposed term $\Delta H_{\text{Solute Inter}}$ of $\Delta H_{\text{Host-Guest}}$, the computed $\Delta H_{\text{Solute Inter (vdW)}}$ and $\Delta H_{\text{Solute Inter (Coul)}}$ show that both force fields model highly similar inter-solute attractions, and the main determinant is from water. Both force fields allow the sugar ring to flip in the free states, and β-CD can easily adjust to an open cavity conformation when forming a complex with a guest. Therefore, unlike existing study showing that substituents attached to decorated β-CDs block a guest from binding (26), the ring flipping itself in our study did not hinder guest binding. However, more flipped sugar rings modeled by GAFF-CD allow the formation of more H-bonds between waters and β-CD as compared with conformations modeled by q4MD-CD. Therefore, with GAFF-CD the cavity more energetically accommodates stable water molecules, which results in large enthalpy penalty from $\Delta H_{\text{Host-Water (Coul)}}$ term on desolvating those water molecules. We suspected that the bonded parameters with GAFF-CD may highly prefer sugar ring flipping in the free states. However, the MD simulations in vacuum showed that both GAFF-CD and q4MD-CD highly prefer wide-open, crystal structure-like conformations in the free states (Fig. S12). Because β-CD is reasonably flexible, in particular with GAFF-CD modeling, adding explicit water molecules easily induces the conformation changes. A “slaving” model in which water drives protein fluctuations was proposed (27). Recently, a direct measurement of hydration water dynamics in protein systems illustrated that the surface hydration-shell fluctuation drives protein side-

chain motions (28). Here we showed that the water molecules are highly responsible for molecular recognition in both thermodynamics and kinetics.

For neutral solutes without long-range electrostatic steering effects, the theoretical k_{on} may be estimated by multiplying the restricted target area by the diffusion-controlled limit $k_{on\_diffuse}$ (29), 2.5% $\times 4 \times 10^{10}$ $M^{-1}s^{-1}$ = 10^9 $M^{-1}s^{-1}$, which is close to the modeled k_{on} of most guests binding with q4MD-CD. The association rate can be faster than the theoretical value if the intermolecular attractions are strong enough to bring the guest that collides onto the host out of the restricted target area to the cavity. This situation can be observed in the sticky binding pathway of the strong binders. k_{on} can also be slower than the theoretical value 10^9 $M^{-1}s^{-1}$ because a guest always needs to compete with water molecules during binding. With GAFF-CD, the desolvation barrier is higher because the complex formation requires breaking of more H-bonds between free β-CD and its solvation shell, resulting in more unsuccessful guest binding and slower k_{on}. This different from an intuition where more β-CD conformational change from sugar ring flipping may seem to slow down k_{on}. In the complex formation, β-CD gained a few kcal/mol, showing a more negative $\Delta H_{Host\ Conf}$ on binding. A similar finding from investigating a binding free energy barriers for a drug binding a protein showed that desolvation of the binding pocket contributes the most to the free energy cost (30). However, for molecular systems that encounter large-scale conformational changes and/or induce fit during ligand binding, rearranging conformations may still significantly affect the association rate constants (31), and the kinetic property can be highly system-dependent. With q4MD-CD, because of a less stable H-bond network, the role of desolvation in binding kinetics is not as important as with GAFF-CD.

Unlike desolvation effects, which are quite different from the two force fields, another dominant but similar driving force for binding is the attractive component of the vdW energy, ranging from -6 to -23 kcal/mol. This driving force may be expected because of the nonpolar property of the β-CD cavity and the neutral guests. This term mainly accounts for dispersion forces between β-CD and guests in the force-field parameters and is similar for both force fields, with a trend that larger guests have more negative $\Delta H_{Solute\ Inter\ (vdW)}$. In experiments, measuring the separate contributions for binding from dispersive interactions and classical hydrophobic effects in aqueous environment is challenging, and the absolute values from the dispersive interactions are not available (32, 33). As compared with the vdW attraction, the Coulombic attraction between β-CD and guests is significantly weak because of the neutral guest molecules and few intermolecular H-bonds. The intermolecular attractions are balanced by desolvation, which results in merely a few kcal/mol net binding enthalpy. One may consider hydrophobic effects as

the major contributions to β-CD and guest recognition (34). Of note, although the pocket of β-CD is non-polar, it is a very tiny cavity, and the rims of β-CD consist of several hydroxyl groups. On binding, ~ 20–25 water molecules were replaced by a larger guest, which agrees with experimental measurement (35) (Table S15). However, not all replaced water molecules are "unhappy". Therefore, although the replaced water molecules also regain water-water attractions in the bulk solvent, there are larger costs to replace the stable water molecules, which results in large desolvation penalty.

The systems did not encounter large solute entropy loss, which contrasts with several existing publications that suggested loss of configuration entropy when a drug binds its target protein (36-38). Unlike most drug-like compounds, which fit tightly to their target protein pocket, our guests only loosely fit in the cavity of β-CD. Therefore, the mobility of β-CD is not reduced considerably by a guest. With GAFF-CD, the hydrated water molecules in the cavity of free β-CD showed an ordered H-bond network and slaved the conformational motions of β-CD. On ligand binding, a bound guest did not form a stable H-bond network with β-CD; thus, β-CD showed a slightly increased flexibility. The guests were also able to form various contacts with β-CD. Similar to alternative contacts provided by the hydrophobic binding pocket of protein systems (39), we did not observe rigidity of β-CD with GAFF-CD.

The enthalpy and entropy balance may follow immediately from $\Delta G = \Delta H - T\Delta S$ (23, 40, 41). Therefore, it has been suggested that the entropy-enthalpy compensation is from a much smaller range of experimentally measured ΔG for a series of ligands than the range of ΔH. Different from most experimental techniques, we computed the entropy and enthalpy terms separately, and still observed the entropy-enthalpy compensation. Our guests were all weak binders and did not have a wide spectrum of ΔG. The computed range of ΔH is in a similar ballpark as ΔG, and the range of $-T\Delta S$ is relatively smaller than ΔG and ΔH. As a result, the enthalpy change mostly governs if a guest is a strong or weak binder. Our calculations reveal the physical basis of larger range of ΔH and more similar $-T\Delta S$. The enthalpy calculations are based on energy functions in the force fields, but the Gibb's entropy formula is based on the distribution of the microstates. Unlike protein systems with numerous rotatable bonds and a larger binding site to mostly enclose a ligand, a guest is not completely confined within the cavity of β-CD, and the host remains highly flexible. Interestingly, $-T\Delta S_{water}$ is similar in both force fields, and is not simply proportional to the size of a guest. Instead, $-T\Delta S_{water}$ relates more to the hydrophilicity of a guest such as 1-propanol, methyl butyrate and aspirin when forming a complex with β-CD. The free guests reduce more entropy of water in their solvation shell, and these solvation waters gain more entropy on guest binding. For q4MD-CD, because the free β-CD generally has a more open cavity, more waters were released on

binding (Table S15). However, the ring flipping conformation modelled by GAFF-CD produces a more structured H-bond network for the first hydration shell. As a result, although fewer water molecules were released on binding, those waters gained more entropy than those of β-CD with q4MD-CD, which resulted in a similar computed $-T\Delta S_{water}$ from both force fields. The results suggest that as in enthalpy, entropy calculations feature a fine balance.

Force-field parameters are critical for accurate modeling and successful prediction (42-45). In this study, we used GAFF for β-CD (GAFF-CD) and for all guests, and q4md-CD, a specialized force field for CDs that combines Amber99SB and GLYCAM04 to match experimental geometries from crystal structures and NMR (46). It is common practice to seek agreement between the calculated and experimental binding affinities/binding free energies for validating and improving the parameters of force fields or solvent models. Using computed thermodynamics and kinetics, both force fields for β-CD showed good agreement with experimental binding affinities, which validated the parameters used. Interestingly, GAFF-CD and q4MD-CD resulted an entropy- and enthalpy-driven binding, respectively. In addition, GAFF-CD yielded better agreement between computed and experimental k_{on}. Using only binding free energy in the training set for parameterization was suggested to risk an incorrect entropy-enthalpy balance; therefore, binding enthalpy needs to be considered for optimizing parameters (25). With continuing growth in computer power, for molecular systems with fast association/dissociation rate constants, we suggest considering computed binding kinetics for validating and optimizing force-field parameters as well. Our studies also showed the importance of and challenge in correctly modeling multiple conformations in which solvent effects may be remarkable and experimental structures are not available. Although our preliminary studies indicated that using TIP3P and TIP4P water models did not yield different sampled conformations during MD simulations, other molecular systems may be more sensitive to the solvent effects with different water models. In the future, we envision a more careful force-field optimization that considers binding free energy, enthalpy-entropy balance and kinetic properties. We also anticipate further investigation into the role of water in the binding kinetics of various guests to a pocket with different polar and/or nonpolar properties (47, 48). This work revealed the role of solvation waters and the detailed balance between enthalpy and entropy driven process. It deepens our comprehension of rational drug design and parameterization.

Methods

We performed microsecond-timescale MD runs for the 7 β-CD cyclodextrin complex systems using published protocol (49). We post-analyzed potential energies for MD runs of each species for 7 systems to compute binding enthalpy (ΔH) and its decompositions. Internal (vibrational and conformational) entropy of β-CD and guest molecules was computed by using Gibbs entropy formula based on well-defined conformations of the molecules. External entropy of the guest molecules was computed by numerical integration over their translational and rotational degrees of freedom using MD trajectory. Water entropy was computed by using grid cell method (50). We computed the binding entropy (ΔS) by summing up solute internal and external entropies, and water entropy. Water entropy was decomposed by translation/rotation and conformation entropy. Two equations were used to calculate binding affinities with computed thermodynamics and kinetic values, $\Delta G_{Comp1} = \Delta H - T\Delta S$, and $\Delta G_{Comp2} = -RT\ln(k_{on} \cdot C^{o} / k_{off})$, respectively. Uncertainties were also evaluated. Details can be found in SI Section 1.

ACKNOWLEDGEMENTS We thank support from the US National Institute of Health (GM-109045), US National Science Foundation (MCB-1350401), and NSF national super computer centers (TG-CHE130009). We also thank Dr. Michael Gilson, Dr. Niel Henriksen and Dr. Ron Levy for discussions on β-cyclodextrin force fields.

References

1. Leavitt S & Freire E (2001) Direct measurement of protein binding energetics by isothermal titration calorimetry. *Curr Opin Struct Biol* 11(5):560-566.
2. Bouchemal K & Mazzaferro S (2012) How to conduct and interpret itc experiments accurately for cyclodextrin-guest interactions. *Drug Discov Today* 17(11-12):623-629.
3. Swinney DC (2009) The role of binding kinetics in therapeutically useful drug action. *Curr Opin Drug Discovery Dev* 12(1):31-39.
4. Schreiber G, Haran G, & Zhou HX (2009) Fundamental aspects of protein-protein association kinetics. *Chem Rev* 109(3):839-860.
5. Pan AC, Borhani DW, Dror RO, & Shaw DE (2013) Molecular determinants of drug-receptor binding kinetics. *Drug Discov Today* 18(13-14):667-673.
6. Guo D, Mulder-Krieger T, Ijzerman AP, & Heitman LH (2012) Functional efficacy of adenosine a2a receptor agonists is positively correlated to their receptor residence time. *Br J Pharmacol* 166(6):1846-1859.
7. Sykes DA, Dowling MR, & Charlton SJ (2009) Exploring the mechanism of agonist efficacy: A relationship between efficacy and agonist dissociation rate at the muscarinic m-3 receptor. *Mol Pharmacol* 76(3):543-551.
8. Friedrichs MS*, et al.* (2009) Accelerating molecular dynamic simulation on graphics processing units. *J Comput Chem* 30(6):864-872.
9. Szejtli J (2013) *Cyclodextrin technology* (Springer Science & Business Media).
10. Rekharsky MV & Inoue Y (1998) Complexation thermodynamics of cyclodextrins. *Chem Rev* 98(5):1875-1917.

11. Fukahori T, Kondo M, & Nishikawa S (2006) Dynamic study of interaction between beta-cyclodextrin and aspirin by the ultrasonic relaxation method. *J Phys Chem B* 110(9):4487-4491.
12. Barros TC, Stefaniak K, Holzwarth JF, & Bohne C (1998) Complexation of naphthylethanols with beta-cyclodextrin. *J Phys Chem A* 102(28):5639-5651.
13. Schneider HJ, Hacket F, Rudiger V, & Ikeda H (1998) Nmr studies of cyclodextrins and cyclodextrin complexes. *Chem Rev* 98(5):1755-1785.
14. Wickstrom L, He P, Gallicchio E, & Levy RM (2013) Large scale affinity calculations of cyclodextrin host-guest complexes: Understanding the role of reorganization in the molecular recognition process. *J Chem Theory Comput* 9(7):3136-3150.
15. Chen W, Chang CE, & Gilson MK (2004) Calculation of cyclodextrin binding affinities: Energy, entropy, and implications for drug design. *Biophys J* 87(5):3035-3049.
16. Jana M & Bandyopadhyay S (2011) Hydration properties of alpha-, beta-, and gamma-cyclodextrins from molecular dynamics simulations. *J Phys Chem B* 115(19):6347-6357.
17. Henriksen NM, Fenley AT, & Gilson MK (2015) Computational calorimetry: High-precision calculation of host-guest binding thermodynamics. *J Chem Theory Comput* 11(9):4377-4394.
18. Koehler JEH & Grczelschak-Mick N (2013) The beta-cyclodextrin/benzene complex and its hydrogen bonds - a theoretical study using molecular dynamics, quantum mechanics and cosmo-rs. *Beilstein J Org Chem* 9:118-134.
19. Liu P, Zhang D, & Zhan J (2010) Investigation on the inclusions of pcb52 with cyclodextrins by performing dft calculations and molecular dynamics simulations. *J Phys Chem A* 114(50):13122-13128.
20. Lambert A, Yeguas V, Monard G, & Ruiz-Lopez MF (2011) What is the effective dielectric constant in a beta-cyclodextrin cavity? Insights from molecular dynamics simulations and qm/mm calculations. *Comp Theor Chem* 968(1-3):71-76.
21. Fukahori T, Nishikawa S, & Yamaguchi K (2004) Kinetics on isomeric alcohols recognition by alpha- and beta-cyclodextrins using ultrasonic relaxation method. *Bull Chem Soc Jpn* 77(12):2193-2198.
22. Nishikawa S, Fukahori T, & Ishikawa K (2002) Ultrasonic relaxations in aqueous solutions of propionic acid in the presence and absence of beta-cyclodextrin. *J Phys Chem A* 106(12):3029-3033.
23. Chodera JD & Mobley DL (2013) Entropy-enthalpy compensation: Role and ramifications in biomolecular ligand recognition and design. *Annu Rev Biophys* 42:121-142.
24. Chang CE & Gilson MK (2004) Free energy, entropy, and induced fit in host-guest recognition: Calculations with the second-generation mining minima algorithm. *J Am Chem Soc* 126(40):13156-13164.
25. Yin J, Fenley AT, Henriksen NM, & Gilson MK (2015) Toward improved force-field accuracy through sensitivity analysis of host-guest binding thermodynamics. *J Phys Chem B* 119(32):10145-10155.
26. Tidemand KD, Schonbeck C, Holm R, Westh P, & Peters GH (2014) Computational investigation of enthalpy-entropy compensation in complexation of glycoconjugated bile salts with beta-cyclodextrin and analogs. *J Phys Chem B* 118(37):10889-10897.
27. Bellissent-Funel MC*, et al.* (2016) Water determines the structure and dynamics of proteins. *Chem Rev* 116(13):7673-7697.
28. Qin YZ, Wang LJ, & Zhong DP (2016) Dynamics and mechanism of ultrafast water-protein interactions. *Proc Natl Acad Sci USA* 113(30):8424-8429.
29. Northrup SH, Allison SA, & McCammon JA (1984) Brownian dynamics simulation of diffusion-influenced bimolecular reactions. *J Chem Phys* 80(4):1517-1526.
30. Mondal J, Friesner RA, & Berne BJ (2014) Role of desolvation in thermodynamics and kinetics of ligand binding to a kinase. *J Chem Theory Comput* 10(12):5696-5705.
31. Wilson C*, et al.* (2015) Using ancient protein kinases to unravel a modern cancer drug's mechanism. *Science* 347(6224):882-886.
32. Persch E, Dumele O, & Diederich F (2015) Molecular recognition in chemical and biological systems. *Angew Chem Int Ed* 54(11):3290-3327.

33. Hobza P (2012) Calculations on noncovalent interactions and databases of benchmark interaction energies. *Acc Chem Res* 45(4):663-672.
34. Snyder PW, Lockett MR, Moustakas DT, & Whitesides GM (2014) Is it the shape of the cavity, or the shape of the water in the cavity? *European Physical Journal-Special Topics* 223(5):853-891.
35. Taulier N & Chalikian TV (2006) Hydrophobic hydration in cyclodextrin complexation. *J Phys Chem B* 110(25):12222-12224.
36. Mobley DL & Dill KA (2009) Binding of small-molecule ligands to proteins: "What you see" is not always "what you get". *Structure* 17(4):489-498.
37. Silver NW*, et al.* (2013) Efficient computation of small-molecule configurational binding entropy and free energy changes by ensemble enumeration. *J Chem Theory Comput* 9(11):5098-5115.
38. Huang Y-mM, Chen W, Potter MJ, & Chang C-eA (2012) Insights from free-energy calculations: Protein conformational equilibrium, driving forces, and ligand-binding modes. *Biophys J* 103(2):342-351.
39. Chang CEA, McLaughlin WA, Baron R, Wang W, & McCammon JA (2008) Entropic contributions and the influence of the hydrophobic environment in promiscuous protein-protein association. *Proc Natl Acad Sci USA* 105(21):7456-7461.
40. Sharp K (2001) Entropy-enthalpy compensation: Fact or artifact? *Protein Sci* 10(3):661-667.
41. Faver JC, Yang W, & Merz KM (2012) The effects of computational modeling errors on the estimation of statistical mechanical variables. *J Chem Theory Comput* 8(10):3769-3776.
42. Beauchamp KA, Lin YS, Das R, & Pande VS (2012) Are protein force fields getting better? A systematic benchmark on 524 diverse nmr measurements. *J Chem Theory Comput* 8(4):1409-1414.
43. Lindorff-Larsen K*, et al.* (2012) Systematic validation of protein force fields against experimental data. *PLoS One* 7(2).
44. Rauscher S*, et al.* (2015) Structural ensembles of intrinsically disordered proteins depend strongly on force field: A comparison to experiment. *J Chem Theory Comput* 11(11):5513-5524.
45. Wickstrom L*, et al.* (2016) Parameterization of an effective potential for protein-ligand binding from host-guest affinity data. *J Mol Recognit* 29(1):10-21.
46. Cezard C, Trivelli X, Aubry F, Djedaini-Pilard F, & Dupradeau F-Y (2011) Molecular dynamics studies of native and substituted cyclodextrins in different media: 1. Charge derivation and force field performances. *PCCP* 13(33):15103-15121.
47. Setny P, Baron R, Kekenes-Huskey PM, McCammon JA, & Dzubiella J (2013) Solvent fluctuations in hydrophobic cavity-ligand binding kinetics. *Proc Natl Acad Sci USA* 110(4):1197-1202.
48. Weiss RG, Setny P, & Dzubiella J (2016) Solvent fluctuations induce non-markovian kinetics in hydrophobic pocket-ligand binding. *J Phys Chem B* 120(33):8127-8136.
49. Fenley AT, Henriksen NM, Muddana HS, & Gilson MK (2014) Bridging calorimetry and simulation through precise calculations of cucurbituril-guest binding enthalpies. *J Chem Theory Comput* 10(9):4069-4078.
50. Gerogiokas G*, et al.* (2014) Prediction of small molecule hydration thermodynamics with grid cell theory. *J Chem Theory Comput* 10(1):35-48.

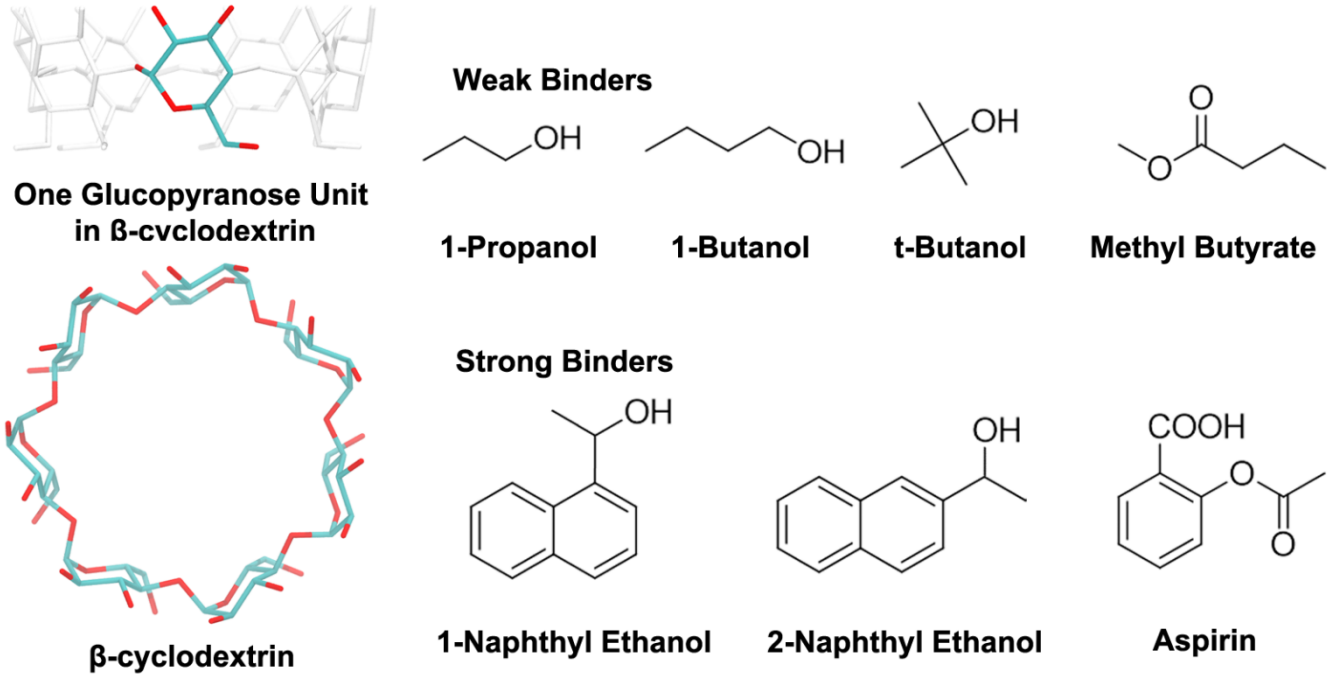

Fig. 1. The structure of β-cyclodextrin (β-CD) and the 7 guest molecules. In the structure of β-CD, hydrogen atoms are not shown.

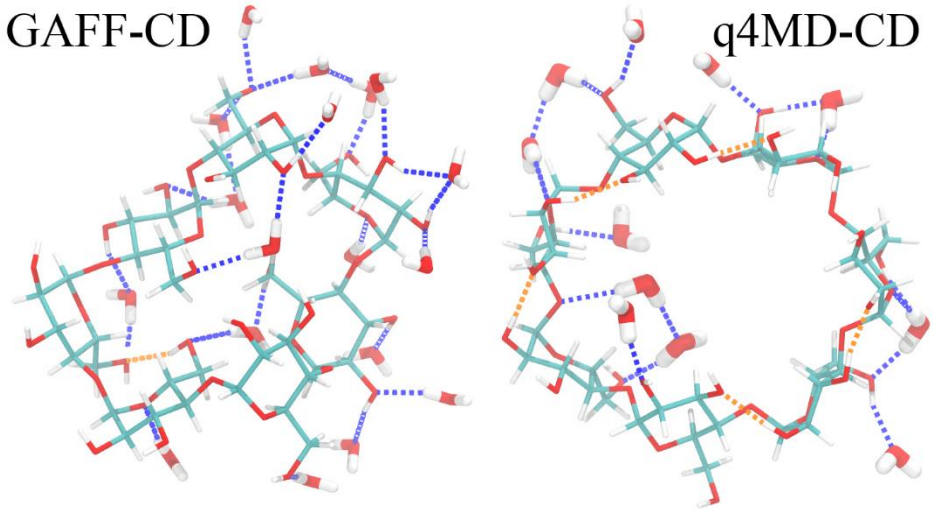

Fig. 2. The hydrogen bond (H-bond) patterns of representative free β-CD conformations with GAFF-CD and q4MD-CD. The numbers of waters H-bonded with β-CD, H-bonds with water (blue dotted lines) and intramolecular H-bonds (orange dotted lines) are18, 24, 1 with GAFF-CD and 11, 16, 5 with q4MD-CD, respectively.

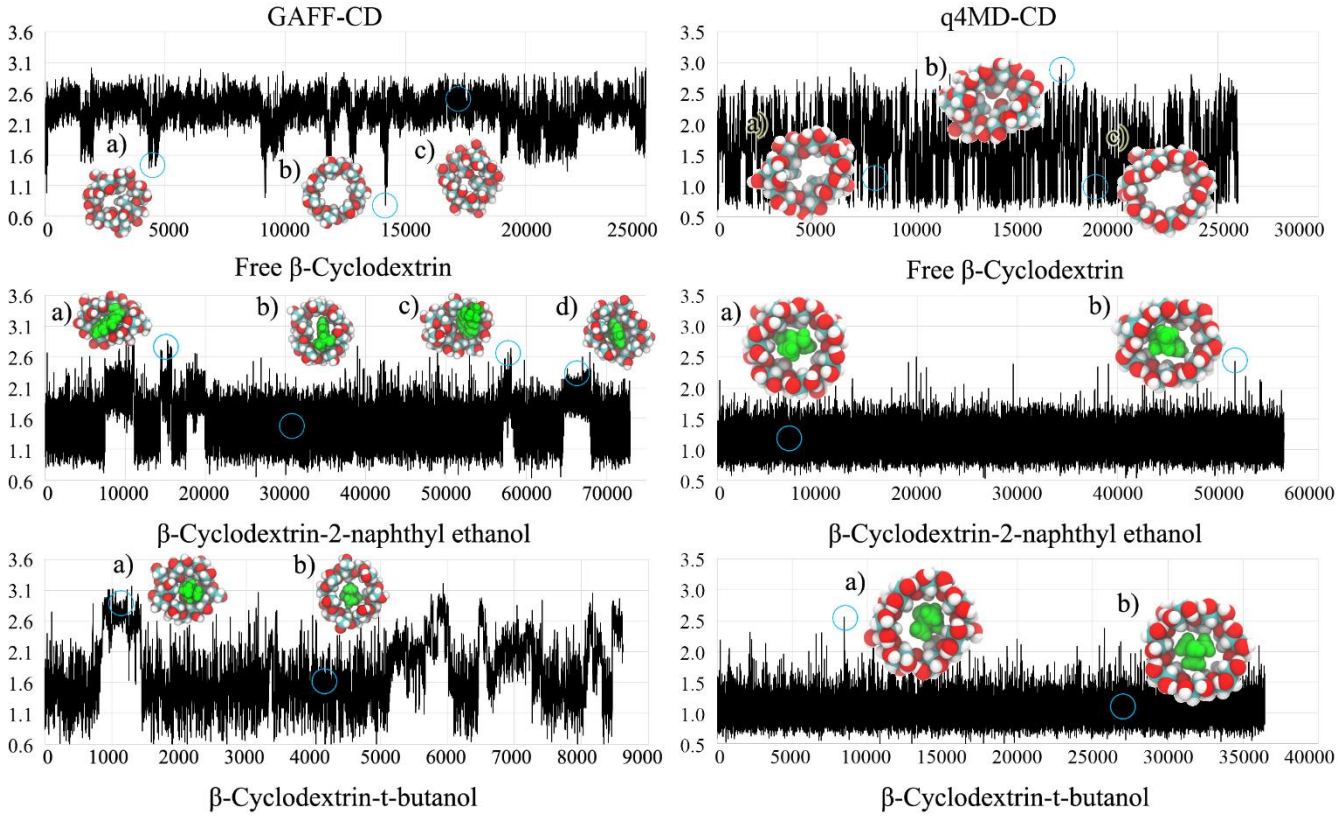

Fig. 3. RMSD plots and representative conformations of β-CD for free β-CD and complexes with 2-naphthyl ethanol and t-butanol with GAFF-CD and q4MD-CD. RMSD (Å) are computed against the crystal structure by using conformations chosen every 100 ps from all conformations of free β-CD and bound-state conformations of complexes. Representative conformations are shown near the labels and circles on the plots. In the representative conformations, ligands are in green.

Table 1. Experimental and computed thermodynamics†

Calculated (GAFF-CD)			
Guest	ΔG_{Comp1}	ΔH	$-T\Delta S$
1-propanol	-1.54±1.37	0.54±1.17	-2.08±0.19
1-butanol	1.01±0.94	2.99±0.88	-1.98±0.06
methyl butyrate	-2.40±0.91	1.88±0.86	-4.29±0.05
t-butanol	0.38±0.82	2.86±0.76	-2.48±0.06
1-naphthyl ethanol	-3.01±0.58	-1.41±0.55	-1.60±0.03
aspirin	-3.84±0.63	-0.01±0.60	-3.83±0.04
2-naphthyl ethanol	-2.93±0.57	-0.88±0.54	-2.05±0.03
Calculated (q4MD-CD)			
Guest	ΔG_{Comp1}	ΔH	$-T\Delta S$
1-propanol	-2.21±0.84	-0.66±0.78	-1.55±0.06
1-butanol	-1.33±0.63	-0.85±0.59	-0.48±0.04
methyl butyrate	-4.17±0.69	-2.00±0.65	-2.17±0.05
t-butanol	-2.50±0.70	-2.87±0.65	0.37±0.05
1-naphthyl ethanol	-5.53±0.61	-5.44±0.57	-0.09±0.04
aspirin	-6.33±0.68	-4.30±0.64	-2.03±0.05
2-naphthyl ethanol	-4.32±0.59	-4.03±0.56	-0.29±0.03
Experimental			
Guest	ΔG	ΔH	$-T\Delta S$
1-propanol	-0.88±0.29	1.43±0.48	-2.34±0.57
1-butanol	-1.67	0.69	-2.34
methyl butyrate	-1.99±0.02	/	/
t-butanol	-2.22±0.01	/	/
1-naphthyl ethanol	-3.22±0.03	/	/
aspirin	-3.74±0.01	/	/
2-naphthyl ethanol	-3.97±0.07	/	/
Units: kcal/mol			

*Experimental standard deviation of 1-butanol is not available.
†Standard deviations are marked by ±.

Table 2. Experimental and computed kinetics†

Calculated (GAFF-CD)			
Guest	k_{on} $M^{-1}s^{-1}$	k_{off} s^{-1}	K_{eq} M^{-1}
1-propanol	$2.0\pm0.1\times10^{8}$	$3.9\pm0.3\times10^{8}$	0.51±0.1
1-butanol	$2.2\pm0.1\times10^{8}$	$1.1\pm0.2\times10^{8}$	2.0±0.3
methyl butyrate	$3.9\pm0.1\times10^{8}$	$8.0\pm0.6\times10^{7}$	4.9±0.4
t-butanol	$2.3\pm0.1\times10^{8}$	$8.5\pm1.2\times10^{7}$	3.2±0.4
1-naphthyl ethanol	$8.6\pm1.1\times10^{8}$	$1.5\pm1.9\times10^{6}$	559±100
aspirin	$1.1\pm0.0\times10^{9}$	$2.4\pm0.3\times10^{7}$	46.±4.3
2-naphthyl ethanol	$9.5\pm0.4\times10^{8}$	$5.2\pm0.9\times10^{6}$	182±23
Calculated (q4MD-CD)			
Guest	k_{on} $M^{-1}s^{-1}$	k_{off} s^{-1}	K_{eq} M^{-1}
1-propanol	$1.2\pm0.0\times10^{9}$	$1.2\pm0.0\times10^{8}$	10.1±0.2
1-butanol	$1.5\pm0.0\times10^{9}$	$3.3\pm0.1\times10^{7}$	46±1.2
methyl butyrate	$1.6\pm0.1\times10^{9}$	$1.1\pm0.1\times10^{7}$	147±15
t-butanol	$1.1\pm0.1\times10^{9}$	$7.2\pm1.0\times10^{6}$	158±18
1-naphthyl ethanol	$1.2\pm0.5\times10^{9}$	$1.4\pm0.5\times10^{6}$	876±42
aspirin	$3.2\pm0.3\times10^{9}$	$3.1\pm0.9\times10^{6}$	1035±83
2-naphthyl ethanol*	3.9×10^{9}	5.0×10^{5}	7788
Experimental			
Guest	k_{on} $M^{-1}s^{-1}$	k_{off} s^{-1}	K_{eq} M^{-1}
1-propanol	$5.1\pm0.7\times10^{8}$	$1.2\pm0.1\times10^{8}$	4.2±0.6
1-butanol	$2.8\pm0.8\times10^{8}$	$3.8\pm0.6\times10^{7}$	7.2±2.0
methyl butyrate	$3.7\pm0.3\times10^{8}$	$1.3\pm0.0\times10^{7}$	29±1
t-butanol	$3.6\pm0.1\times10^{8}$	$8.5\pm0.1\times10^{6}$	42.6±1.0
1-naphthyl ethanol	$4.7\pm1.9\times10^{8}$	$4.8\pm1.8\times10^{5}$	230±10
aspirin	$7.2\pm0.0\times10^{8}$	$1.3\pm0.0\times10^{6}$	549±2
2-naphthyl ethanol	$2.9\pm1.6\times10^{8}$	$1.8\pm0.7\times10^{5}$	820±90

*The standard deviations of rate constants of β-CD-2-naphthyl ethanol with q4MD-CD are not available because of lack of adequate binding events.

†Standard deviations are marked by ±.

Table 3. Decomposition of computed entropy*

Guest	Calculated (GAFF-CD)					Calculated (q4MD-CD)				
	$-T\Delta S_{Water}$	$-T\Delta S_{Host}$	$-T\Delta S_{Guest\ Int}$	$-T\Delta S_{Guest\ Ext}$	$-T\Delta S$	$-T\Delta S_{Water}$	$-T\Delta S_{Host}$	$-T\Delta S_{Guest\ Int}$	$-T\Delta S_{Guest\ Ext}$	$-T\Delta S$
1-propanol	-3.32±0.18	-0.52±0.01	0.00±0.00	1.75±0.00	-2.08±0.19	-3.36±0.05	0.21±0.00	0.02±0.00	1.57±0.00	-1.55±0.06
1-butanol	-2.37±0.06	-1.20±0.00	-0.05±0.00	1.64±0.00	-1.98±0.06	-2.31±0.03	0.25±0.00	-0.17±0.00	1.74±0.00	-0.48±0.04
methyl butyrate	-4.00±0.04	-1.58±0.00	-0.10±0.00	1.39±0.00	-4.29±0.05	-4.12±0.04	0.22±0.00	-0.11±0.00	1.84±0.00	-2.17±0.05
t-butanol	-2.22±0.05	-1.84±0.00	0.00±0.00	1.57±0.00	-2.48±0.06	-1.84±0.05	0.45±0.00	0.00±0.00	1.76±0.00	0.37±0.05
1-naphthyl ethanol	-2.28±0.02	-1.24±0.00	0.00±0.00	1.92±0.00	-1.60±0.03	-2.17±0.03	0.12±0.00	0.00±0.00	1.95±0.01	-0.09±0.04
aspirin	-4.08±0.03	-1.53±0.00	0.12±0.00	1.67±0.00	-3.83±0.04	-3.81±0.04	0.11±0.00	-0.16±0.00	1.82±0.00	-2.03±0.05
2-naphthyl ethanol	-2.33±0.02	-1.33±0.00	0.00±0.00	1.61±0.01	-2.05±0.03	-2.31±0.03	0.03±0.00	0.00±0.00	1.99±0.01	-0.29±0.03
Units: kcal/mol										

*$-T\Delta S_{Water}$, $-T\Delta S_{Host}$, $-T\Delta S_{Guest\ Int}$, $-T\Delta S_{Guest\ Ext}$ and $-T\Delta S$ are the entropy change of water, internal entropy change of β-cyclodextrin, internal and external entropy change of guests, and the total binding entropy at 298K. All values are in kcal/mol. Standard deviations are marked by ±.

Table 4. Decomposition of computed solute-water interaction*

Guest	Calculated (GAFF-CD)						Calculated (q4MD-CD)					
	$\Delta H_{Host-Water}$			$\Delta H_{Guest-Water}$			$\Delta H_{Host-Water}$			$\Delta H_{Guest-Water}$		
	Total	vdW	Coul	Total	vdW	Coul	Total	vdW	Coul	Total	vdW	Coul
1-propanol	12.2	1.34	10.85	6.92	2.12	4.8	13.72	4.08	9.63	7.74	3.85	3.89
1-butanol	20.55	0.12	20.44	8.34	4.15	4.19	17.72	5.45	12.27	9.21	4.99	4.22
methyl ethanol	25.58	0.64	24.94	10.28	5.79	4.49	22.05	6.51	15.54	11.1	6.34	4.77
t-butanol	20.71	-1.38	22.09	8.39	4.16	4.23	16.31	4.75	11.56	7.87	5.12	2.75
1-naphthyl ethanol	35.45	0.91	34.54	14.93	9.62	5.32	29.65	8.63	21.02	14.51	9.6	4.91
aspirin	34.6	0.4	34.2	19.15	9.13	10.02	28.91	7.75	21.16	18.17	9.35	8.82
2-naphthyl ethanol	33.21	1.54	31.66	13.76	9.29	4.47	28.82	8.95	19.87	13.95	9.37	4.59
Units: kcal/mol												

*$\Delta H_{Host-Water}$ and $\Delta H_{Guest-Water}$ decompose into van der Waals energy ($\Delta H_{Host-Water}$ (vdW) and $\Delta H_{Guest-Water}$ (vdW)) and Coulombic energy ($\Delta H_{Host-Water}$ (Coul) and $\Delta H_{Guest-Water}$ (Coul)) terms. All values are in kcal/mol.